Journal of the European Ceramic Society 38 (2018) 2279–2288

Contents lists available at ScienceDirect

Journal of the European Ceramic Society

journal homepage: www.elsevier.com/locate/jeurceramsoc

Original Article

Tribological behavior of α^1/β^1-SiAlON-TiN composites

Nurcan Calis Acikbas

Department of Metallurgical and Materials Engineering, Bilecik S.E. University, Bilecik, Turkey

ARTICLE INFO

Keywords:
α^1:β^1-SiAlON-TiN composites
Tribology
Wear mechanisms
Microstructure
Cutting tool

ABSTRACT

There are limited studies on the tribological properties of SiAlON-TiN composites. Therefore, in the present study, tribology tests were conducted on a number of α^1/β^1-SiAlON-TiN composites with different α^1/β^1-SiAlON phase ratio and TiN content, fabricated with unique compositional design. The influence of α^1/β^1-SiAlON phase ratios, microstructure, mechanical properties and TiN content on friction and wear behavior was investigated and wear mechanisms were explained. Tribology tests were conducted on computer controlled tribometer under dry unlubricated ambient conditions with a linear reciprocating movement in a ball-on-disc sliding wear configuration and test parameters kept as constant. It was observed that TiN addition (17 wt.%) did not change the friction (CoF) of SiAlON and wear rate and wear volume were observed to increase. Wear mechanisms showed differences with α^1:β^1-SiAlON phase ratio. Fracture toughness had very pronounced effect on wear resistance.

1. Introduction

Alumina based (Al_2O_3-SiC_w) and silicon nitride based (Si_3N_4-SiC/TiC/TiN) ceramic matrix composites have been used for cast iron and superalloy machining. SiAlONs are structured in the fundamental unit of Si_3N_4 and they are basically defined as solid solution between the Si_3N_4 and Al_2O_3. They possess many inherent advantageous over Si_3N_4 such as easy sintering, wide compositional design (100%wt.α to 100% wt. β), different intergranular phase chemistry, microstructure and hence wide range of mechanical and physical properties [1]. SiAlON ceramics have been also used for super alloy machining [2]. However their performance is not as effective as Al_2O_3-SiC_w cutting tools especially at higher cutting speeds. On the other hand Al_2O_3-SiC_w cutting tools have many disadvantages over SiAlON ceramics such as costly production method and SiC whiskers are dangerous to human health. Therefore if the performance of SiAlON ceramics is improved, they will be good competitors to Al_2O_3-SiC_w cutting tools with cost advantage.

Insufficient chemical durability of SiAlON ceramics inhibited wide use of it for superalloys machining. The chemical durability of SiAlONs can be improved in two possible ways: proper compositional design with optimum z (solid solution) value, crystalline intergranular phase (IGP), good coalescence behavior of IGP and addition of second phases. Increasing z value (~1) leads to longer tool life because of the reduced chemical wear during machining [3]. However with the increase of z value to ~1, mechanical properties like fracture toughness and hardness will deteriorate [4,5]. Therefore the z value should be optimized and the incorporation of second phases in order to improve chemical resistance is more feasible. TiN is a very good candidate to improve chemical wear resistance and mechanical properties of SiAlON ceramics [6–11]. On the other hand compositional design is very crucial that effect chemical wear resistance of α^1/β^1-SiAlONs, especially, at high temperatures. The SiAlON samples should have high z value (0.5 <) and crystalline intergranular phase chemistry and good coalescence behavior to resist the high temperatures during superalloy machining. In our previous studies, the effect of cation type, intergranular phase (IGP) amount and cation mole ratios on z value and intergranular phase crystallization of α^1/β^1-SiAlON-TiN composites and the effect of z value on the crystallization and coalescence of IGP were investigated [12–14]. It was found that crystallization tendency of Er and Yb cations were higher than that of Y cation. The highest fracture toughness 7.4 $MPam^{1/2}$ and moderate hardness values (15.37 GPa) was obtained with Er containing composition. It was concluded that, z value was an effective parameter on intergranular phase chemistry and crystallization after sintering. Post sintering heat treatment improved the crystallization and consequent coalescence behavior of IGP.

Since the friction and wear are the important factors during machining, the investigation of the tribological behavior of α^1/β^1-SiAlON-TiN composites is crucial. Studies on tribological behavior of Si_3N_4-TiN composites have been widely reported [15–19]. It was reported that incorporation of TiN phase increase wear resistance and with the formation of titanium oxide solid lubricant film reduce friction [20–23]. However, there are limited studies on the tribological properties of SiAlON-TiN composites [24]. Therefore, in the present study, tribology tests were conducted on a number of

α^1/β^1-SiAlON and α^1/β^1-SiAlON-TiN composites with different α^1/β^1-SiAlON phase ratio and TiN content, fabricated with unique

E-mail address: nurcan.acikbas@bilecik.edu.tr.

https://doi.org/10.1016/j.jeurceramsoc.2018.01.013
Received 25 July 2017; Received in revised form 2 January 2018; Accepted 11 January 2018
Available online 12 January 2018
0955-2219/

Table 1
Specifications of prepared SiAlON-TiN composites.

Sample Code	TiN content (wt%)	α′: β′ -SiAlON Phase Ratios	Bulk Density (g/cm^3)	Theoretical Density (g/cm^3)	Theoretical Density %
T0035	0	35 α′ : 65 β′	3.3592	3.3693	99.70
T1735	17	35 α′ : 65 β′	3.5796	3.5885	99.75
T2510	25	10 α′ : 90 β′	3.6854	3.6939	99.77
T2575	25	75 α′ : 25 β′	3.6851	3.6921	99.81

compositional design. The influence of α′:β′-SiAlON phase ratios, microstructure, mechanical properties and TiN content on friction and wear behavior were investigated and wear mechanisms were explained.

2. Experimental procedures

α′:β′-SiAlON-TiN composites were developed with different α′:β′-SiAlON phase ratios (10α′:90β′, 35α′:65β′ and 75α′:25β′) and containing various amounts of TiN particles (17 and 25wt%). α′:β′-SiAlON compositions were designed with 9Er:0.5Sm:0.5Ca cation system and 0.6 of z value (see Table 1). In our previous study [14], crystalline and good coalescence behavior of IGP, high aspect ratio grains over 7 and hence the highest fracture toughness 7.4 MPam$^{1/2}$ and moderate hardness values (15.37GPa) was obtained with 9Er:05:Sm:0.5Ca cation system. If the material has this kind of composition, it should exhibit better mechanical and chemical properties during superalloy machining. The coding for the compositions is as follows: the first three figures represent the TiN content. T17 means 17 wt.% TiN content. The next two figures represent the α′-SiAlON phase ratios.

UBE-E10 grade α-Si_3N_4 powder (1.4 wt% O content, UBE Co. Ltd., Japan), high purity AlN powder (1.6 wt% O, H Type, Tokuyama Corp. Japan), Al_2O_3 (Alcoa A16-SG, Pittsburgh, USA), Er_2O_3 (> 99.99%, Treibacher, Austria), Sm_2O_3 (> 99.9%, Stanford Materials Corp., USA), $CaCO_3$ (> 99.75%, Reidel-de Haen, Germany) and TiN powder with average particle size of 1–2 μm (> 99% pure, H.C. Starck, Grade C, Berlin, Germany) were used in order to produce α′β′-SiAlON-TiN composites. The designed compositions were prepared by planetary milling for 90 min at 300 rpm in isopropyl alcohol using Si_3N_4 balls. The milling conditions of nitride based powders would affect the subsequent microstructure and mechanical properties, and these milling conditions were specifically choosen [25]. TiN was introduced into the starting powder mixture in order to provide homogeneous dispersion of TiN particles in the SiAlON matrix. Rotary evaporator was used for drying slurries and then the powders were dry sieved with a mesh size of 150 μm. The powders were uniaxially pressed under 25 MPa, and subsequently cold isostatically pressed at 300 MPa. The pellets were sintered using a two-step gas pressure sintering cycle. The first step (pre-sintering) was carried out at 1890 °C for 60 min at 0.5 MPa nitrogen gas pressure followed by a sintering step at 1940 °C for 60 min at 2.2 MPa nitrogen gas pressure and then the furnace was allowed to cool at a rate of 5 °C/min in order to obtain crystalline IGP.

Archimedes principle was used to measure the bulk density of the samples after sintering by using the following equation.

$$\text{Bulk Density} = \frac{W_1}{W_3 - W_2} x\rho_{water} \quad (1)$$

where, W_1 is dry weight, W_2 is wet weight suspended in water, W_3 is wet weight, B.D. is bulk density. Theoretical density of the samples was found by He gas picnometer (Micromeritics Accupyc II 1340 model) and theoretical density% values were calculated with the following equation.

$$\%\ \text{Theoretical Density} = (\text{Bulk density} / \text{Theoretical density}) * 100 \quad (2)$$

The α′:β′-SiAlON phase ratios and intergranular phase chemistry were determined by X-ray diffraction methods (XRD-Panalytical, Empyrean with Cu-Kα radiation). The α′:β′-SiAlON phase ratios were found by quantitative estimation from the XRD patterns using the integrated intensities of the (102) and (210) reflections of α′-SiAlON and the (101) and (210) reflections of β′-SiAlON by the following equation:

$$\frac{I_\beta}{I_\beta + I_\alpha} = \frac{1}{1 + K[(1/w_\beta) - 1]} \quad (3)$$

where I_α *and* I_β are observed intensities of α′ and β′-SiAlON peaks, respectively, w_β is the relative weight fraction of β′-SiAlON, and K is the combined proportionality constant resulting from the constants in the two equations:

$$I_\beta = K_\beta * W_\beta \quad (4)$$

$$I_\alpha = K_\alpha * W_\alpha \quad (5)$$

K was taken as 0518 for β (101) – α (102) reflections and 0544 for β (210) – α (210) reflections [26].

The cell parameters of β′-SiAlON were measured with silicon powders as the internal standard. The z-value of the β′-SiAlON phase was obtained from the mean of z_a and z_c values given by the following equations:

$$z_a = \frac{a - 7.6044}{0.031} \quad (6)$$

$$z_c = \frac{c - 2.9075}{0.026} \quad (7)$$

where *a* and *c* are the calculated unit cell dimensions of β′-SiAlON: JCPDS card 33–1160 was used as a reference for β-Si_3N_4 where a = 7.6044(2)Å and c = 2.9075(1)Å. z value of all of the developed α′:β′-SiAlON-TiN composites were found between 0.6-0.62. Scanning electron microscopy (SEM) analysis was conducted for microstructural investigations (SEM-ZEISS Supra 40VP) with back-scattered electron imaging mode.

Vickers hardness tests were conducted under 98 N load. The Vickers hardness (HV) was calculated by the following equation (Evans and Charles): [27]

$$HV_{10} = 0.47P/a2 \quad (8)$$

where, HV_{10} is the Vickers hardness, P is load applied and a is half the length of the diagonal of the indentation produced by the indenter. Indentation fracture toughness (K_{1C}) was calculated by the hardness tests using the formula proposed by Niihara et al for median cracks: [28]

$$K_{IC} = 0018 * HV * a^{0,5} * (E/HV)^{0,4} * (c/a - 1)^{-0,5} (\text{for } c/a < 3.5 \text{ and } l/a < 2.5) \quad (9)$$

where 2a is the average indent diagonal length (μm), 2c is the crack length (from one crack tip to another), E is the elastic modulus (GPa) which is taken as a constant equivalent to 320 GPa for all the samples and H is the measured hardness (GPa). The crack length and indent diagonal were measured from optical images of the indented surfaces. 3 samples tested for each composition with 5 indents and the standard deviation was calculated.

Before tribology tests, the sample surfaces was polished and cleaned with acetone in an ultrasonic bath for 10 min and then the samples dried at room temperature. MarSurf PS1 (Mahr GmbH, Gottingen, Germany) model surface profilometer was used to determine surface roughness. Tribological behavior of samples was conducted on computer controlled tribometer (TRD Engineering, Sakarya, Turkey) under dry unlubricated ambient conditions with a linear reciprocating movement in a ball-on-disc sliding wear configuration. The samples were placed on a translation plate, which oscillated at the required stroke length and desired frequency. The coefficient of friction was

found from on-line measured tangential force. The test conditions were kept constant for all of the samples (stroke length: 2 mm, frequency: 10 Hz, sliding distance: 1000 m, normal load: 10 N) for comparison. 3 measurements were taken for each sample. Si_3N_4 ball (TCQ grade, Toshiba, Japan) with 10 mm diameter, z:0.3, E:310 GPa, HV10: 15.5 GPa, Kıc: 4.7 $MPam^{1/2}$) was used as a counter body.

After tribology tests, the wear scar profiles on each sample were measured by laser surface profilometer. 2-D wear scar profiles were extracted from different locations on 3-D profiles and the wear volumes were calculated by integrating the surface area of each 2-D profile over the distance of worn surfaces. The specific wear rate calculated, wear volume (V) divided by load (N) and wear distance (L) as given in Eq. (10);

$$W = \frac{V}{F.L} \tag{10}$$

The worn surfaces were examined by scanning electron microscopy using a Zeiss Supra 40VP model FEG-SEM. EDX analysis were carried out by a Bruker XFlash5010 model EDX detector, mounted on this SEM, in order to determine the chemical composition of the tribofilm As the determination of the TiO_2 content is an important issue in this study, matrix correction from the EDS software were taken into account such as the effects of atomic number, absorption and secondary fluorescence. The local peak to background (P/B) ratios was used as input into the modified ZAF matrix correction. In this case, the P/B-ZAF analysis was used for self-calibrating.

3. Results and discussion

3.1. The effect of TiN incorporation on tribological behavior of SiAlON ceramics

In order to investigate the effect of TiN reinforcement on tribological behavior of SiAlON ceramics, α^1 to β^1-SiAlON phase ratio was kept constant as $35\alpha^1$:$65\beta^1$ and T0035 and T1735 compositions were used for comparison. As seen from the graphics, coefficient of frictions (CoFs) of the developed T0035 and T1735 compositions were very close (0.59 for T0035 and 0.60 for T1735) to each other (Fig. 1). In literature it was stated that CoF values of Si_3N_4-TiN composites changed between 0.3–1.2 depending on test conditions, material properties (hardness, toughness etc.) and particle size of reinforcement phase (nano or micro) [9,20]. The CoF values of developed T0035 and T1735 composition were in the range of these values. The CoF graph of T1735 showed fluctuation up to 500 m and then attained to a steady state condition. The reason of instability of the graph might result from the coarse TiN grains in the microstructure. Presumably, during the first 500 m sliding distance TiO_2 self-lubricating tribofilm formed on the surface, and for this reason the friction coefficient was relatively low. As sliding distance increased, with the wear of SiAlON grains a SiO_2 rich reaction layer would form as in the case of T0035 composition but without TiN, and CoF value would not change. Both TiO_2 and SiO_2 layers contributed to the decrease of friction coefficient value of silicon nitride based ceramics [29–31]. SiO_2 and TiO_2 formation on the worn surface was determined with SEM-EDS analysis, to be discussed in wear mechanism section. In literature the CoF value of SiAlON ceramics are known to be affected by α^1:β^1-SiAlON phase ratios, hardness, fracture toughness, microstructure and surface roughness [29,32]. The α^1:β^1-SiAlON phase ratios, hardness and fracture toughness of T0035 and T1735 compositions were similar but with the addition of TiN particles surface roughness value of T1735 increased 5.5 fold (Table 2). It was revealed that the increase in surface roughness led to an increase in the friction coefficient. In literature similar results were observed in the work of other researchers [33,34].

Table 2, represents the properties of developed materials and their relation to tribological properties. The fracture toughness and hardness values of samples were near each other but with the addition of TiN particles surface roughness value increased 5.5 fold. Incorporation of TiN particles led to an increase in wear volume and wear rate (%20) due to increase in surface roughness. Surface roughness increased due the coarse grain sizes of TiN powder (~1–4 microns) (see Fig. 2). Apart from surface roughness, TiN grain size and TiO_2 tribolayer characteristics also affected the tribological properties. In literature it is stated that wear resistance increases with the addition of TiN into Si_3N_4 matrix [15]. Generally, TiO_2 tribofilm was effective in reducing both friction and wear [9]. However, in this study, TiO_2 tribofilm did not reduce the wear rate. If the tribolayer was easily removed or nonuniform this meant it did not provide any protection [29]. In our case tribolayer was not uniform enough for T1735 and this was not a positive effect on wear resistance. On the other hand, microstructure affected the wear rate. Due to large grain size of TiN phase, more material loss could take place and the wear rate increased. But still both samples were in the range of 10^{-4} mm^3 wear volume which indicated that the samples were in mild wear regime [35].

Material removal processes of developed material during tribology tests of SiAlON/Si_3N_4 and SiAlON-TiN/Si_3N_4 tribo-couples were formation of reaction layer and fracture of this layer, plastic deformation and grain pull-out (Figs. 3 and 4,). The characteristic wear features are marked on the SEM images. During motion of two bodies, grains were

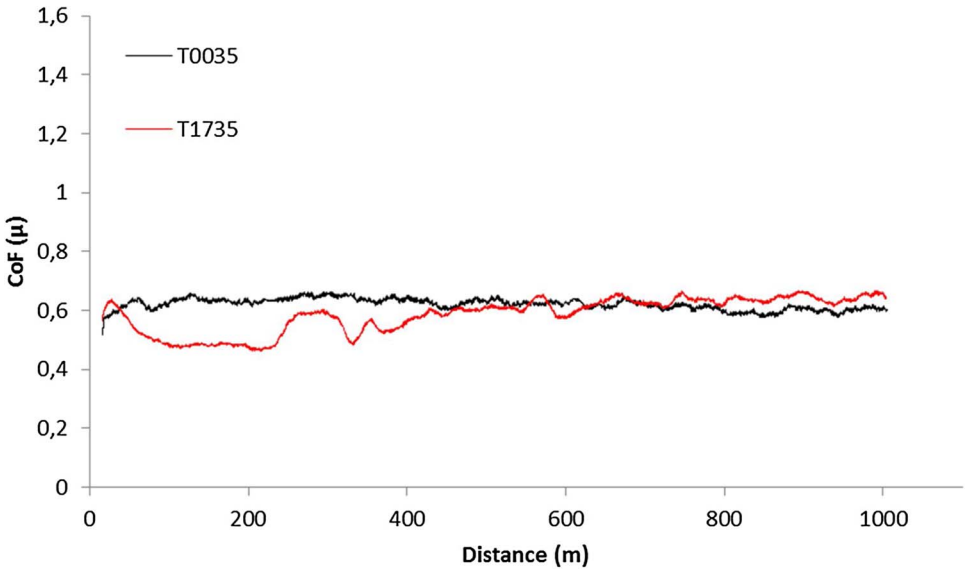

Fig. 1. Plot of frictional behavior of investigated T0035 and T1735 compositions.

Table 2
Specifications of T0035 and T1735 samples.

Sample	α^1:β^1 ratios	Surface roughness	μ	Kıc (MPa $m^{1/2}$)	HV_{10} (GPa)	Wear Rate (mm^3/Nm)	Wear Volume (mm^3)
T0035	65β:35α	0,02	0,59	6,20 ± 0,4	15,73 ± 0,11	$2{,}574 \times 10^{-8}$	$2{,}574 \times 10^{-4}$
T1735	65β:35α	0,13	0,60	6,55 ± 0,1	15,87 ± 0,29	$3{,}0712 \times 10^{-8}$	$3{,}0712 \times 10^{-4}$

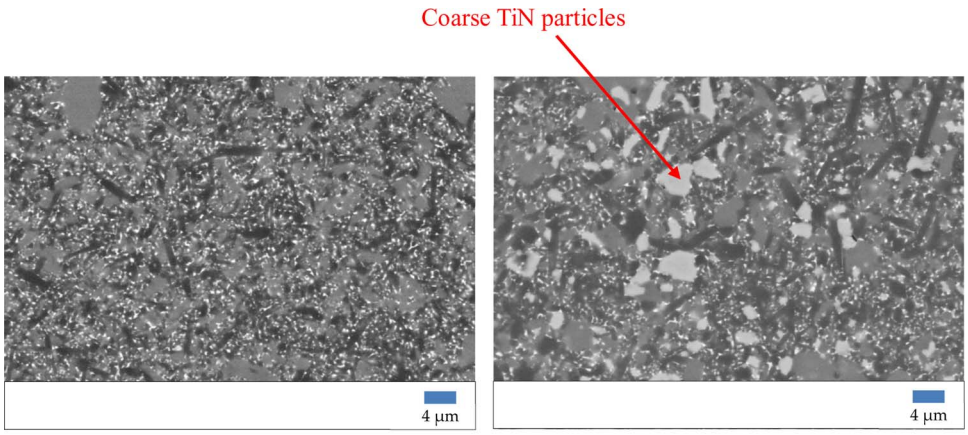

Fig. 2. Representative SEM-BSE images of (a) T0035 and (b) T1735 samples.

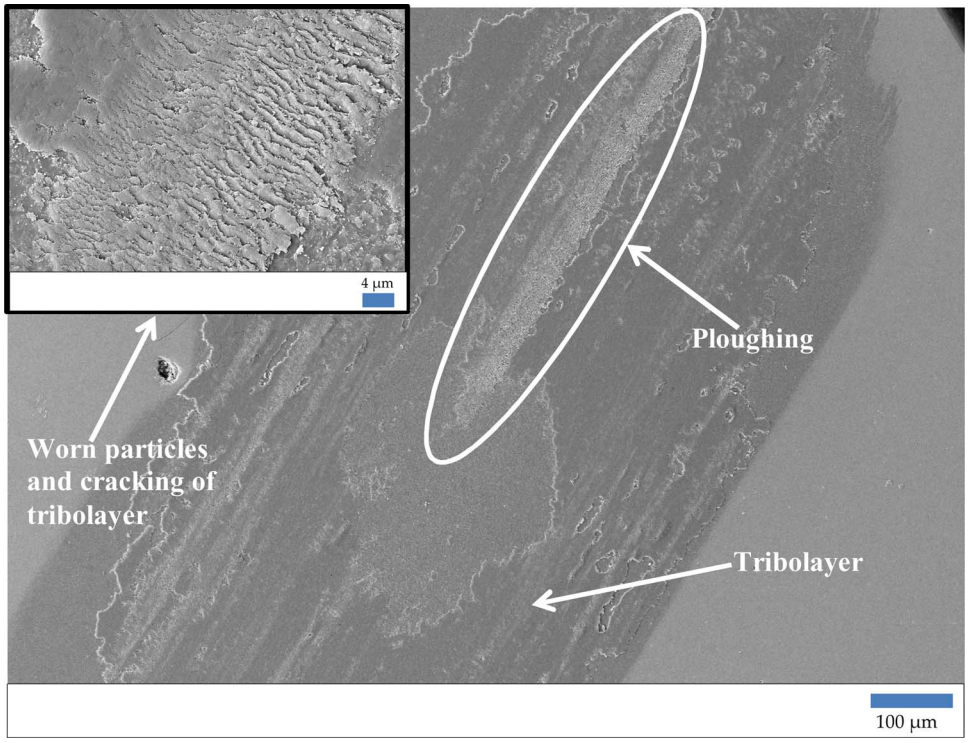

Fig. 3. SEM-SE images of T0035 sample overall and detailed feature of wear scar.

broken for a certain period of time and they accumulated due to motion and heat on the surface of the sample and this resulted in reaction layer formation. Deep cavities in the central region were observed in these materials after the tribology test. Since the motion of ball on the sample surface, plastic deformation was observed and this led to deep cavities in the center of contact region. Less abrasion was observed in other regions different from the central region of the wear scar. The wear resistance of the material significantly was governed by the formation of the tribolayer, the deformation characteristics and fracture of this layer. These features were related to microstructure (grain size, intergranular phase: nature, composition, porosity etc.) and mechanical properties such as hardness and fracture toughness. Since the microstructural properties and hardness and fracture toughness values of both samples were similar, wear mechanisms and tribolayer features were analogous (Figs. 3 and 4).

Tribochemical layer of T0035 and T1735 was characterized with SEM-EDX analysis (Figs. 5 and 6,). Si, O and Al elements were observed for T0035 sample while Ti, Si, O and Al elements were detected for TiN incorporated T1735 coded composition. According to EDX analysis of T0035, SiO_2 rich (74.16 wt.%) tribolayer was formed. Apart from SiO_2 a

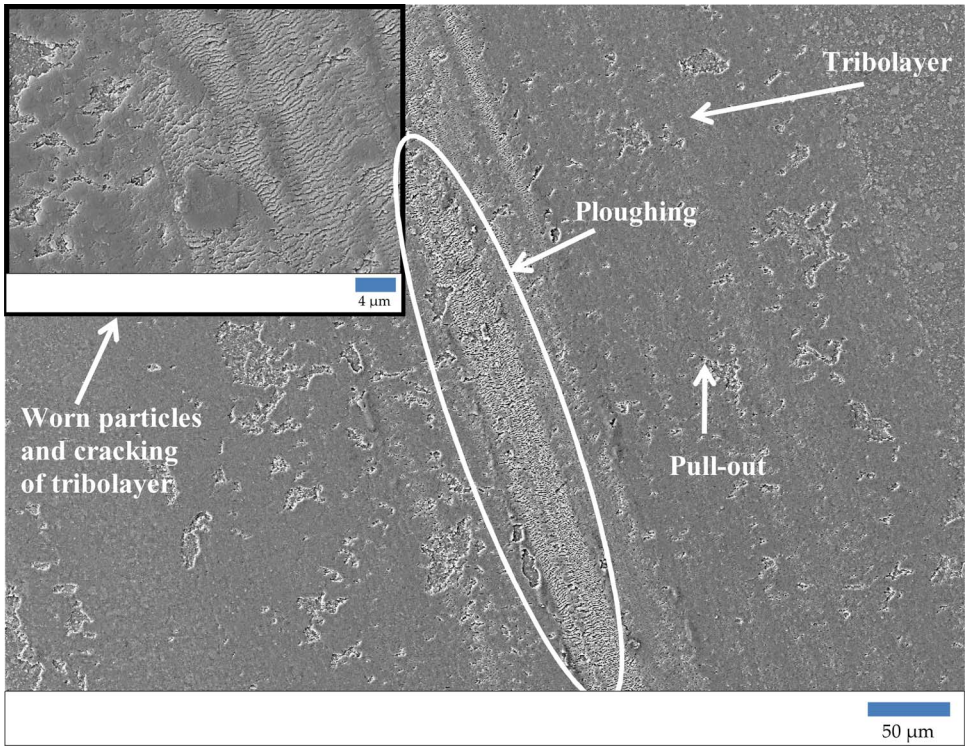

Fig. 4. SEM-SE images of T1735 sample overall and detailed feature of wear scar.

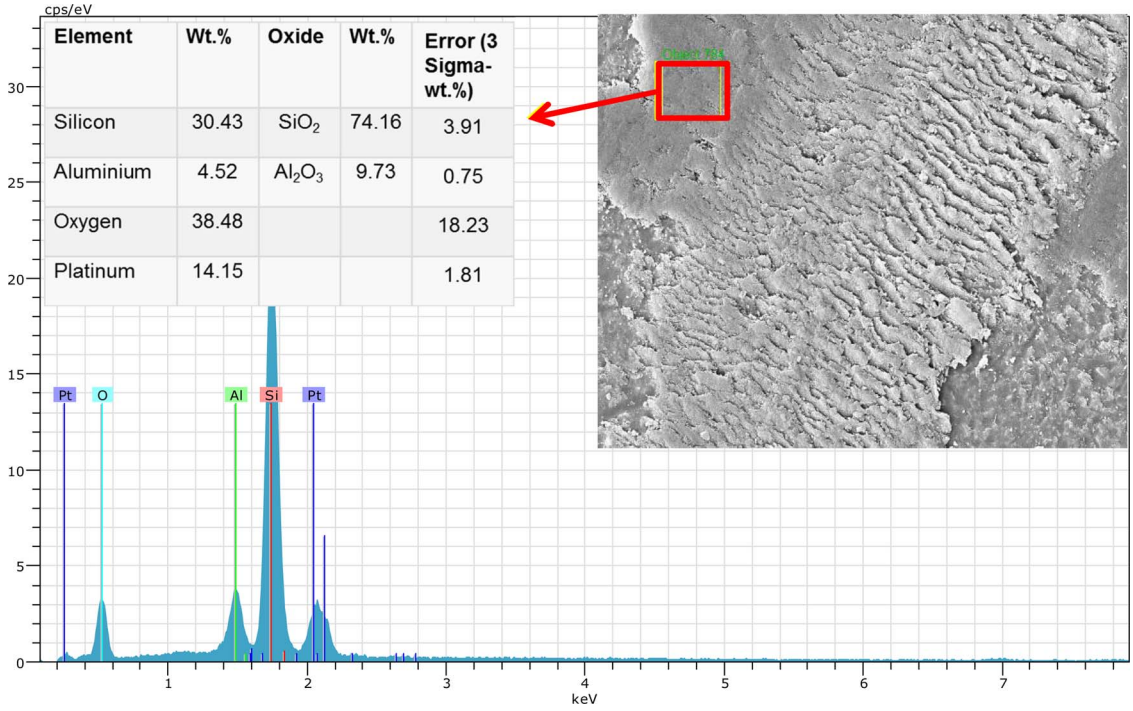

Fig. 5. SEM-EDS analysis of T0035 sample's reaction layer.

minor amount of Al_2O_3 (9.73 wt.%) was present in tribolayer since the SiAlON grains consisted of Al (Fig. 5). Detection of light elements such as oxygen and nitrogen with accuracy was a difficult task. Therefore ZAF correction was used in order to observe the errors. In Fig. 5 the oxygen content was found as 38.48 wt.% with a standard deviation of 18.23 wt.% (3 sigma) for T0035. On the other hand, oxygen content was determined as 42.49 wt.% and the standard deviation was 17.33wt. % (3 sigma) (see Fig. 6) for T1735. The obtained results showed that deviations for oxygen determination were very close to each other (18.23 and 17.33 wt.%). Therefore calculated SiO_2, TiO_2 and Al_2O_3 contents of tribolayer compositions had nearly the same errors. Since both samples had crystalline intergranular phase (Fig. 7) which was harder than the amorphous intergranular phase, tribolayer did not contain elements (such as Er, Sm and Ca) that came from IGP. In my previous study [32], it was found that the second important parameter that affected the wear was characterized by IGP chemistry. If the SiAlONs have amorphous IGP, a thick and protective reaction layer forms. This layer shows lubrication effect and a decrease in the wear rate.

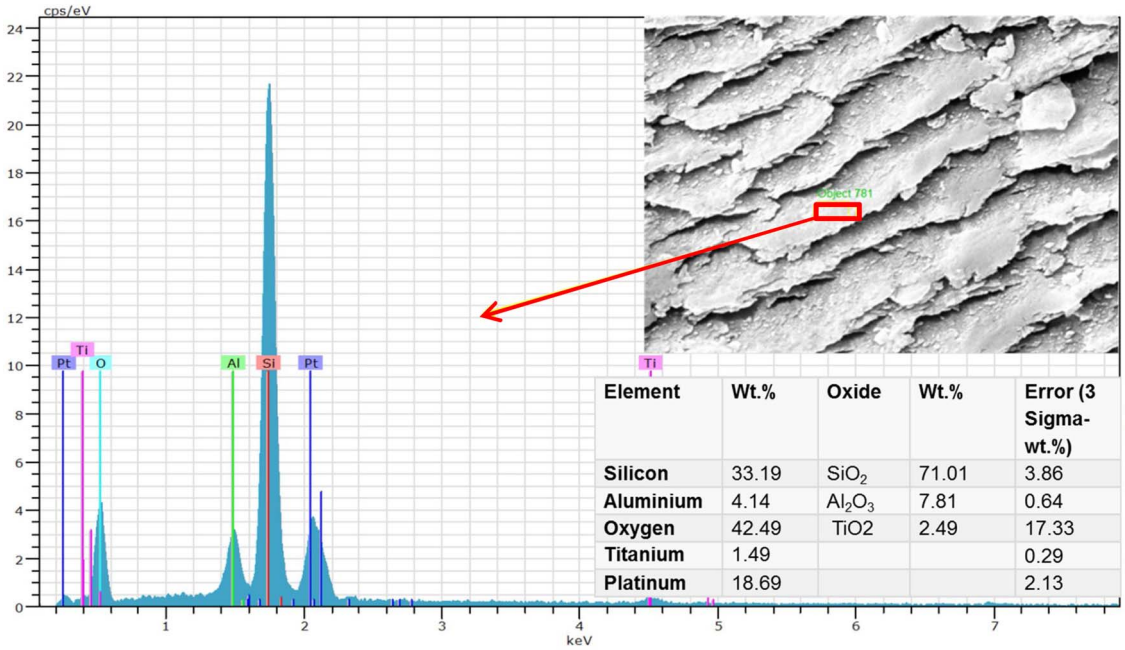

Element	Wt.%	Oxide	Wt.%	Error (3 Sigma-wt.%)
Silicon	33.19	SiO_2	71.01	3.86
Aluminium	4.14	Al_2O_3	7.81	0.64
Oxygen	42.49	TiO2	2.49	17.33
Titanium	1.49			0.29
Platinum	18.69			2.13

Fig. 6. SEM-EDS analysis of T1735 sample's reaction layer.

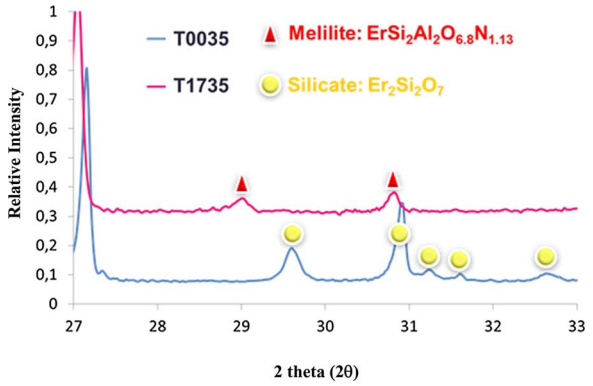

Fig. 7. XRD analysis which shows the IGP of developed T0035 and T1735 samples.

However, for high temperatures amorphous IGP has not been preferred since it melts and deteriorates the high temperature properties.

During the wear tests the reaction layer formed by the wear of SiAlON and TiN grains due to friction causing heat, stress, and grain pull-out. Due to the solid lubrication effect of TiN particles, TiO_2 tribochemical reaction layer was formed (Fig. 6). TiO_2 content (2.49%wt.) of tribolayer was very low compared to SiO_2 amount (71.01 wt%) since the matrix was SiAlON. Apart from TiO_2 and SiO_2, 7.81 wt.% Al_2O_3 was present. Pt peak belonged to electro-conductive coating before SEM-EDX analysis.

3.2. The effect of α′:β′-SiAlON phase ratio on tribological behavior of SiAlON-TiN composites

T2575 and T2510 compositions with 25wt% TiN and different α′:β′-SiAlON phase ratio were used in order to evaluate the effect of α′:β′-SiAlON phase ratio on tribological behavior of SiAlON-TiN composites. Properties of α′:β′-SiAlON-TiN (25wt.%) composites with different α′:β′-phase ratios are given in Table 3.

As the increase of β′-SiAlON phase content (25→90), fracture toughness increased at a rate of about 40%, hardness decreased slightly (%4) and wear rate decreased 3 folds, and hence the wear resistance improved. The microstructural images of T2575 and T2510 were given in Fig. 8. For both compositions TiN particles dispersed in SiAlON matrix homogeneously. The grain size of TiN particles was in the range between 1 to 4 microns. Coarse α′-SiAlON grains (light gray color) with a size between 5–10 microns, and fine, elongated β′-SiAlON grains (dark gray color) existed in the microstructure of T2575 (Fig. 8a). A number of fine elongated β′-SiAlON grains and coarse α′-SiAlON grains were present in T2510 composition (Fig. 8b). The elongated grains helped the increase in fracture toughness. Although TiN content was the same in both compositions, surface roughness was different due to different α′:β′-SiAlON phase ratios (samples polished at the same time). T2575 sample had low surface roughness a rate of almost 50% than T2510.

The CoF graphics of T2575 and T2510 samples were given in Fig. 9. Almost up to 500m, fluctuations were observed in friction coefficient graphs. T2575 sample which had higher α′-SiAlON phase showed higher CoF values than T2510. Study of Satoh et all. revealed similar results with this study [36]. It was explained that, hydration and oxidation reactions were limited in α′-SiAlON ceramics since cations entered the crystal structure of α′-SiAlON and hence this prevented tribolayer formation which could reduce friction coefficient. While T2575 sample had higher hardness value (16.57 GPa) than T2510 (15.90 GPa), the CoF values of T2575 was higher than T2510. As a result, it was concluded that the increase in α′-SiAlON phase ratio led to the increase

Table 3
Properties of α′:β′-SiAlON-TiN (25wt.%) composites with different α′:β′-phase ratios.

Sample	α′:β′ ratios	Surface roughness	μ	Kıc (MPa $m^{1/2}$)	HV_{10} (GPa)	Wear Rate (mm^3/Nm)	Wear Volume (mm^3)
T2575	75α:25β	0,056	0,64	5,85 ± 0,05	16,57 ± 0,23	$6{,}3977 \times 10^{-8}$	$6{,}3977 \times 10^{-4}$
T2510	10α:90β	0,107	0,60	8,20 ± 0,30	15,90 ± 0,03	$2{,}1888 \times 10^{-8}$	$2{,}1888 \times 10^{-4}$

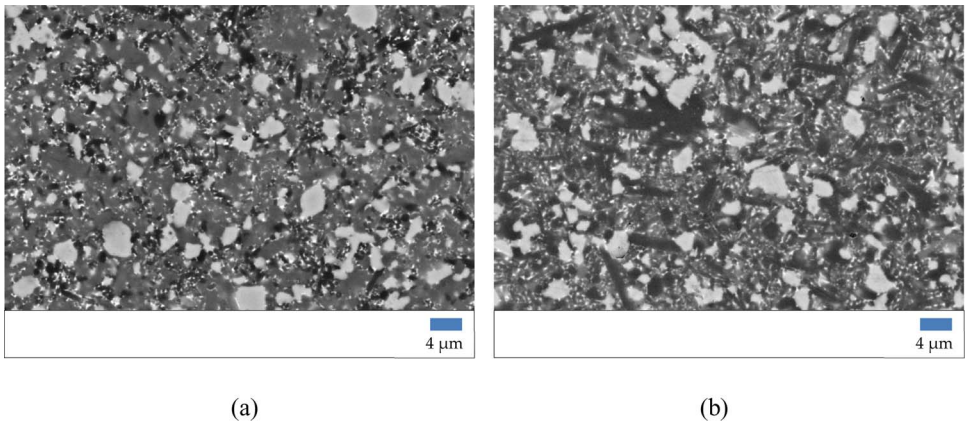

Fig. 8. Representative SEM-BSE images of (a) T2575 and (b) T2510 samples.

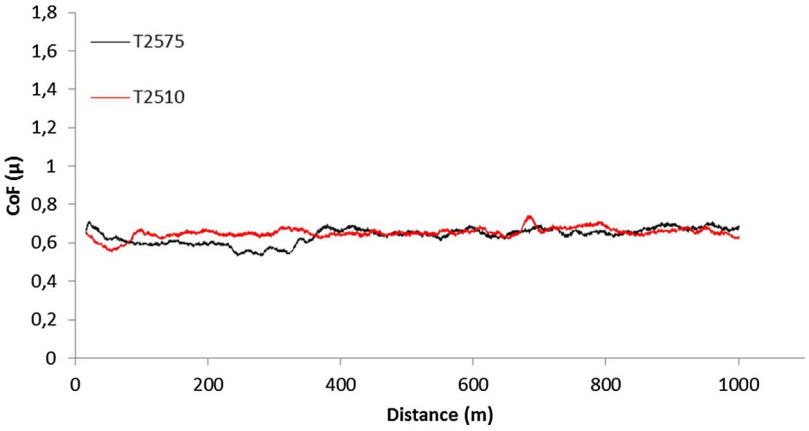

Fig. 9. Plot of frictional behavior of investigated T2510 and T2575 samples.

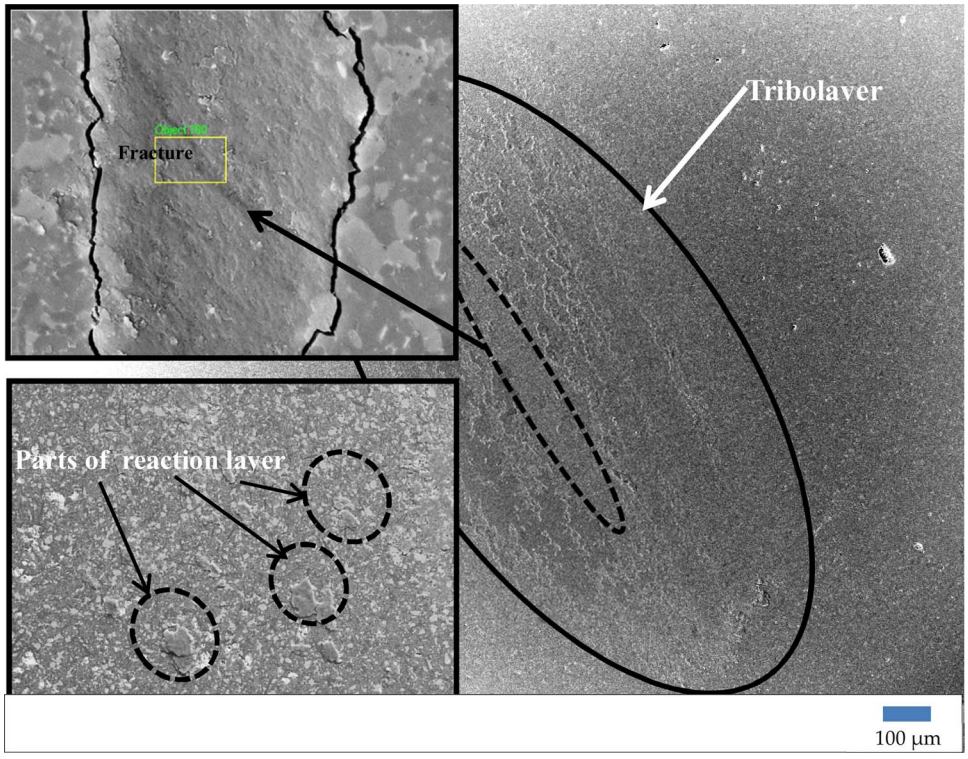

Fig. 10. SEM images of T2575 sample overall and detailed feature of wear scar.

in CoF value and α^{1}:β^{1}-SiAlON phase ratio had more pronounced effect than surface roughness on the CoF.

In literature it was observed that with decrease in CoF value, wear rates decreased [37–39]. A similar phenomenon was observed in this study. As the friction coefficient decreased from 0.64 to 0.60, wear rate decreased almost 3 folds.

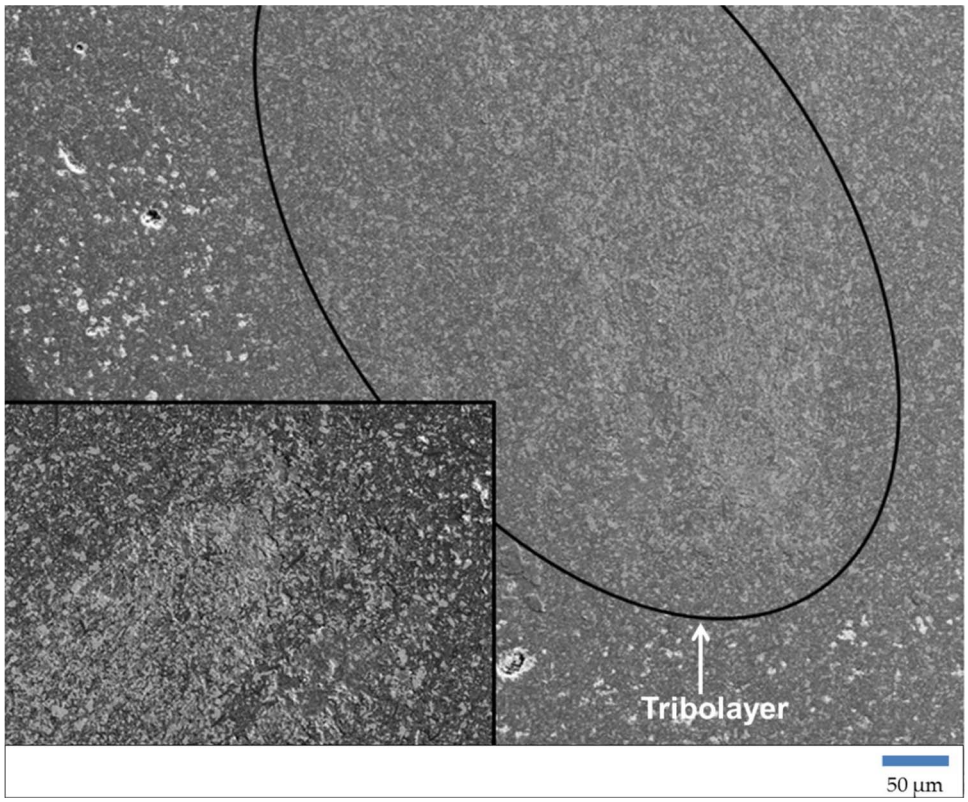

Fig. 11. SEM images of T2510 sample overall and detailed feature of wear scar.

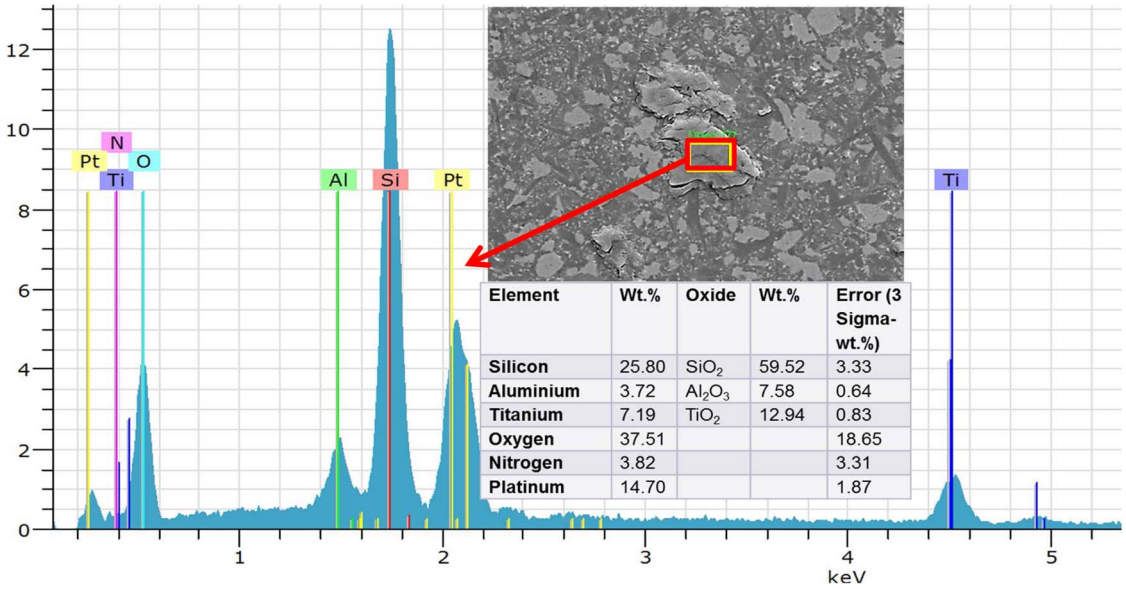

Element	Wt.%	Oxide	Wt.%	Error (3 Sigma-wt.%)
Silicon	25.80	SiO_2	59.52	3.33
Aluminium	3.72	Al_2O_3	7.58	0.64
Titanium	7.19	TiO_2	12.94	0.83
Oxygen	37.51			18.65
Nitrogen	3.82			3.31
Platinum	14.70			1.87

Fig. 12. SEM-EDX spectra which is taken from T2510 sample's tribolayer.

T2510 sample had high fracture toughness and hence showed high wear resistance. In my previous study, it was observed that the fracture toughness was the most important parameter that affected the wear resistance of SiAlON ceramics [32]. If the SiAlON sample had a fracture toughness of $\sim 3\,MPam^{1/2}$, higher material loss took place with the formation of subsurface cracks in the material. Therefore it was concluded that the toughness of the material to be used in wear applications should have been higher than 4 $MPam^{1/2}$ for preventing of subsurface cracking and excessive material loss. In literature it was stated that high values of the ratio of fracture toughness to hardness of materials caused less wear [40].

T2510 had fine α'-SiAlON grains in the β'-SiAlON matrix with elongated (aspect ratio > 7) and fine grains (Fig. 8). Grain size had important effects on wear. Because fine grain size led to both less material loss and formation of reaction layer which was broken in the form of fine grains, and hence the wear resistance improved. Also, if the grain size was small, the number of cracks which formed during wear test, meeting the triple junctions was more, and the crack propagation direction changed, slowing down the rate of crack growth, and hence less material loss took place. Since micro tensions/stresses at the grain boundaries for fine grained material easily removed compared to the coarse grained structures, grain pull-out was prevented. Besides, starting of micro cracking was harder in fine grained microstructures. Dogan and Hawk revealed that if the Si_3N_4 grain size was coarse, more

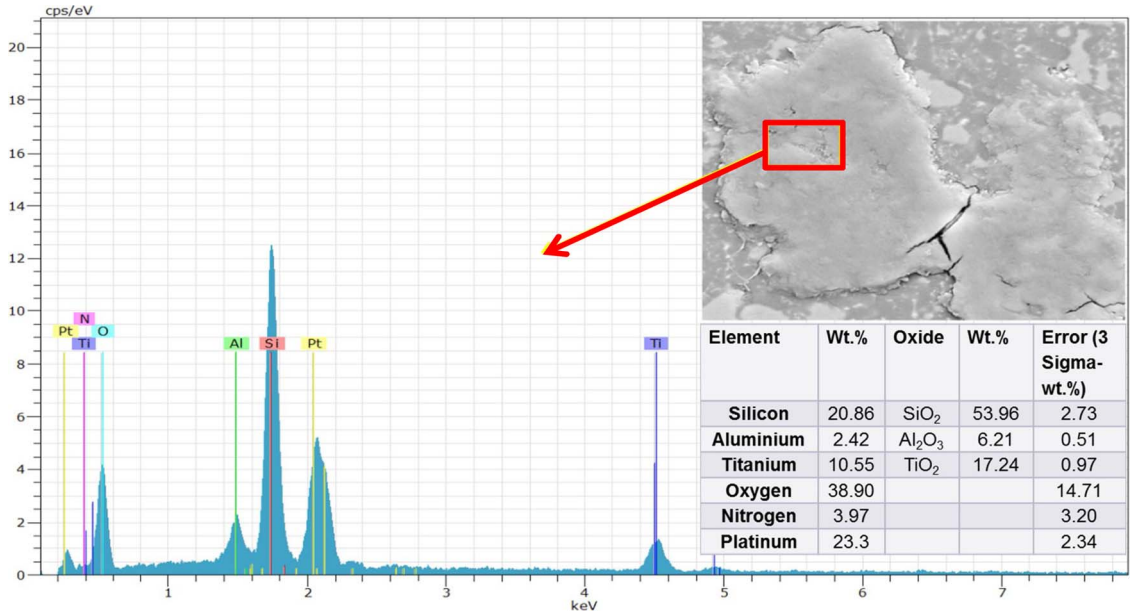

Element	Wt.%	Oxide	Wt.%	Error (3 Sigma-wt.%)
Silicon	20.86	SiO_2	53.96	2.73
Aluminium	2.42	Al_2O_3	6.21	0.51
Titanium	10.55	TiO_2	17.24	0.97
Oxygen	38.90			14.71
Nitrogen	3.97			3.20
Platinum	23.3			2.34

Fig. 13. SEM-EDX spectra which is taken from T2575 sample's tribolayer.

volume of material was lost per grain removed [41].

Comparing to tribolayer features of T2575 and T2510, α^1-SiAlON rich composition (T2575) had comparatively less reaction layer than T2575. Because hydration and oxidation reactions were limited in α^1-SiAlON ceramics, cations entered the crystal structure of α^1-SiAlON, causing the formation of only a thinner tribolayer. T2575 sample showed intergranular fracture where the stress was high in the contact region due to relatively low fracture toughness Even so both samples had thin and fragile reaction layer characteristic (see Figs. 10 and 11). More TiO_2 formation (17.24%) was observed in T2575 composition than T2510 (12.94%) (see Figs. 12 and 13). Because the grain size of T2510 was finer than T2575, the reaction layer was broken in the form of finer grains and less material loss occurred. It was observed that fracture toughness had a very pronounced effect on the wear rate. Differences in fracture toughness value resulted in change in wear mechanisms. Plastic deformation was not observed in T2510 which had high fracture toughness while intergranular fracture was present in T2575.

4. Conclusions

SiAlON and SiAlON-TiN composites with different α^1:β^1-SiAlON phase ratios (10α^1:90β^1, 35α^1:65β^1, 75α^1:25β^1) and containing various amounts of TiN particles (17 and 25wt%) were developed. The effect of TiN addition into SiAlON matrix, TiN content and α^1:β^1-SiAlON phase ratio of SiAlON matrix on tribological behavior were investigated and following conclusions were reached:

- TiN addition (17 wt%) did not change the friction (CoF) of SiAlON and increase in wear rate and wear volume (%20) were observed. This can be resulted from the increase in surface roughness of ~5.5 folds. Microstructure had an important effect on wear rate. Due to large grain size of TiN phase, more material loss was observed and so the wear rate increased.
- α^1:β^1-SiAlON phase ratios had effect on surface roughness of samples. Less tribolayer formation was obtained in α^1-SiAlON rich composition and higher CoF value was observed.
- As the friction coefficient decrease from 0.64 to 0.60, wear rate decreased almost 3 folds in 25wt.% TiN containing compositions.
- Grain size had important effect on wear. Because fine grain size led to both less material loss and formation of reaction layer which was broken in the form of fine grains, and hence the wear resistance improved.
- The wear rate increased or decreased with increasing TiN content depending on α to β^1-SiAlON phase ratio. If the material had high β^1-SiAlON content, the material showed high fracture toughness and was more wear resistant.
- It was observed that fracture toughness had very pronounced effect on wear rate and differences in fracture toughness value resulted in the change of wear mechanisms. Plastic deformation was not observed in T2510 which had high fracture toughness while intergranular fracture existed in T2575.

Acknowledgement

The samples were produced in the scope of TUBITAK CARIER-110M727 Project (Project Manager: Assoc. Prof. Dr. Nurcan CALIS ACIKBAS) for which the author thanks to TUBITAK (Ankara, Turkey) for financial support.

References

[1] B. Bitterlich, S. Bitsch, K. Friederich, SiAlON based ceramic cutting tools, J. Eur. Ceram. Soc. 28 (2008) 989–994.
[2] I.A. Choudhury, M.A. El-Baradie, Machinability of nickel-base super alloys: a general review, J. Mater. Process. Technol. 77 (1998) 278–284.
[3] H. Mandal, F. Kara, S. Turan, A. Kara, Novel SiAlON ceramics for cutting tool applications, Key Eng. Mater. 237 (2003) 193–202.
[4] G. Brandt, Wear and Thermal Shock Resistant SiAlON Cutting Tool Material, U.S. Patent No. 5,965, 471, 1999.
[5] P.K. Mehrotra, R.D. Nixon, J.L. Swiokla, High z SiAlON and Cutting Tools Made Therefrom and Method of Using, International Application Published Under the Patent Cooperation Treaty (PCT), WO 94/12317, 9 June, 1994.
[6] E. Ayas, A. Kara, H. Mandal, S. Turan, F. Kara, Production of α-β SiAlON–TiN/TiCN composites by gas pressure sintering, Silic. Indus. 69 (2004) 287–292.
[7] R.G. Duan, G. Roebben, J. Vleugels, O. Biest, Optimization of microstructure and properties of insitu formed β-O-SiAlON–TiN composite, Mater. Sci. Eng. A 427 (2006) 195–202.
[8] T. Ekström, P.O. Olsson, β-SiAlON ceramics with TiN particle inclusions, J. Eur. Ceram. Soc. 13 (6) (1994) 551–559.
[9] I. Schulz, M. Herrmann, I. Endler, I. Zalite, B. Speisser, J. Kreusser, Nano Si3N4 composites with improved tribological properties, Lub. Sci. 21 (2009) 69–81.
[10] J. Tatami, E. Kodama, H. Watanabe, H. Nakano, T. Wakihara, K. Komeya, T. Megiro, A. Azushima, Fabrication and wear properties of TiN nanoparticle dispersed Si_3N_4 ceramics, J. Ceram. Soc. Jap. 116 (2008) 749–754.
[11] A. Bellosi, A. Fiegna, A. Giachello, Microstructure and Properties of Electrically Conductive Si_3N_4–TiN Composites, Elsevier Science Publishers B.V., 1991, pp. 225–234.

[12] N. Calis Acikbas, O. Demir, The effect of cation type, intergranular phase amount and cation mole ratios on z value and intergranular phase crystallisation of SiAlON ceramics, Ceram. Int. 39 (2013) 3249–3259.
[13] N. Calis Acikbas, S. Tegmen, S. Ozcan, G. Acikbas, Thermal shock behaviour of α:β SiAlON-TiN composites, Ceram. Int. 40 (2014) 3611–3618.
[14] N. Calis Acikbas, F. Kara, The effect of z value on intergranular phase crystallization of α:β-SiAlON-TiN composites, J. Eur. Ceram. Soc. 37 (2017) 923–930.
[15] M. Hadad, G. Blugan, J. Kubler, E. Rosset, L. Rohr, J. Michler, Tribological behaviour of Si_3N_4 and Si_3N_4–TiN based composites and multi-layer laminates, Wear 260 (2006) 634–664.
[16] Blugan, G., Kubler, J. Critical Flaw Size Reduction in Commercial Si_3N_4-TiN Composites for Wear Applications, EMPA, Swiss Federal Laboratories for Materials Testing and Research, Laboratory for High Performance Ceramics. http://www.gruppofrattura.it/ocs/index.php/ICF/ICF11/paper/view/9905/9317.
[17] G. Blugan, M. Hadad, T. Graulea, J. Kuebler, Si_3N_4–TiN–SiC three particle phase composites for wear applications, Ceram. Int. 40 (2014) 1439–1446.
[18] B. Zou, C. Huang, J. Song, H. Liu, Ho, Zhu, Cutting performance and wear mechanism of Si_3N_4-based nanocomposite ceramic cutting tool in machining of cast iron, Mach. Sci. Technol. 15 (2) (2011) 192–205.
[19] A. Skopp, M. Woydt, K.-H. Habig, Tribological behavior of silicon nitride unlubricated sliding between 22°C materials under and 1000°C, Wear 181–183 (1995) 571–580.
[20] Y. Imada, The tribological reaction accompanying friction and wear of silicon nitride containing titanium nitride, Trans. ASME 114 (1992) 230–235.
[21] Z. Da-Ming, A comparative study on the microstructure and tribological properties of Si_3N_4 and TiN films produced by the IBED method, Tribol. Int. 29 (6) (1996) 507–513.
[22] F. Brenscheidt, S. Oswald, A. Mücklich, E. Wieser, W. Möller, Wear mechanisms in titanium implanted silicon nitride ceramics, Nucl. Instrum. Methods Phys. Res. Sect. B. 129 (1997) 483–486.
[23] C. Melandri, M.G. Gee, G. de Portu, S. Guicciardi, High temperature friction and wear testing of silicon nitride ceramic, Tribol. Int. 28 (1995) 403–413.
[24] Y.S. Zhaoa, Y. Yanga, J.T. Lia, I.P. Borovinskaya, K.L. Smirnov, Combustion synthesis and tribological properties of SiAlON based ceramic composites, Int. J. Self-Propag. High-Temp. Synth. 19 (3) (2010) 172–177.
[25] S. Ozcan, G. Acikbas, N. Ozbay, N. Calis Acikbas, The effect of silicon nitride powder characteristics on SiAlON microstructures, densification and phase assemblage, Ceram. Int. 43 (13) (2017) 10057–10065.
[26] K. Liddell, X-Ray Analysis of Nitrogen Ceramic Phases. MSc. Thesis, University of Newcastle, Upon Tyne, UK, 1979.
[27] A.G. Evans, E.A. Charles, Fracture toughness determinations by indentation, J. Am. Ceram. Soc. 59 (1976) 371–372.
[28] K. Niihara, R. Morena, P.H. Hasselman, Evaluation of Kıc of brittle solids by the indentation method with low crack-to-indent ratios, J. Mater. Sci. Lett. 1 (1982) 13–16.
[29] R. Kumar, N. Calis Acikbas, F. Kara, H. Mandal, B. Basu, Microstructure – mechanical properties – wear resistance relationship of SiAlON ceramics, Metall. Mater. Trans. A (2009) 2319–2332.
[30] A.K. Mallik, K.M. Reddy, N. Calis Acikbas, F. Kara, H. Mandal, D. Basu, B. Basu, Influence of SiC addition on tribological properties of SiAlON, Ceram. Int. (2011) 2495–2504.
[31] A. Kumar Mallik, N. Calis Acikbas, F. Kara, H. Mandal, D. Basu, A comparative study of SiAlON ceramics, Ceram. Int. (2012) 5757–5767.
[32] N. Calis Acikbas, Development of SiAlON Ceramics for Tribological Applications, PhD. Thesis Anadolu University, 2009.
[33] N. Umehara, K. Kato, The effect of initial surface roughness on friction of self-mating silicon nitride in water, J. Jpn. Soc. Tribol. 42 (11) (1997) 879–885.
[34] K. Kato, K. Adachi, Wear of advanced ceramics, Wear 253 (2002) 1097–1104.
[35] S.M. Hsu, M. Shen, Wear prediction of ceramics, Wear 256 (2004) 867–878.
[36] T. Satoh, S. Sakaguchi, K. Hirao, M. Toriyama, S. Kanzaki, Influence of Al-O-Y solid solution on the aqueous tribological behavior of Si_3N_4, J. Am. Ceram. Soc. 84 (2001) 462–464.
[37] W.G. Zhang, W.M. Liu, H.W. Liu, L.G. Yu, Q.J. Xue, Tribological behaviors of (Ca, Mg)-SiAlON under lubrication of polyols, Wear 223 (1998) 143–149.
[38] W.G. Zhang, W.M. Liu, H.W. Liu, L.G. Yu, Friction and wear behaviors of a (Ca,Mg)–SiAlON/SAE 52100 steel pair under the lubrication of various polyols as water-based lubricating additives, Tribol. Int. 33 (2000) 769–775.
[39] D.A. Rani, Y. Yoshizawa, M.I. Jones, H. Hyuga, K. Hirao, Y. Yamauchi, Comparison of tribological behaviour between α-SiAlON/Si_3N_4 and Si_3N_4/Si_3N_4 sliding pairs in water lubrication, J. Am. Ceram. Soc. 88 (2005) 1655–1658.
[40] M.A. Moore, F.S. King, Abrasive wear of brittle solids, Wear 60 (1) (1980) 123–140.
[41] C.P. Doğan, J.A. Hawk, Microstructure and abrasive wear in silicon nitride ceramics, Wear 250 (2001) 256–263.